Biomed Microdevices (2013) 15:617–626
DOI 10.1007/s10544-013-9781-9

Biocompatible TiO_2 nanoparticle-based cell immunoassay for circulating tumor cells capture and identification from cancer patients

Rongxiang He · Libo Zhao · Yumin Liu · Nangang Zhang · Boran Cheng · Zhaobo He · Bo Cai · Sizhe Li · Wei Liu · Shishang Guo · Yong Chen · Bin Xiong · Xing-Zhong Zhao

Published online: 19 June 2013

Abstract We demonstrate the isolation of circulating tumor cells (CTCs) with a biocompatible nano-film composed of TiO_2 nanoparticles. Due to the enhanced topographic interaction between nano-film and cancer cell surface, cancer cells (HCT116) spiked into PBS and healthy blood can be recovered from the suspension, whose efficiencies were respectively 80 % and 50 %. Benifit from the biocompatibility of this nano-film, *in-situ* culture of the captured cancer cells is also available, which provides an alternative selection when the capture cell number was inadequate or the sample cannot be analyzed immediately. For the proof-of-concept study, we use this nano-film to separate the circulating tumor cells from the colorectal and gastric cancer patient peripheral blood samples and the captured CTCs are identified by a three-colored immunocytochemistry method. We investigated the cancer cells capture strength at the nano-bio interface through exposing the cells to fluid shear stress in microfluidic device, which can be utilized to increase the purity of CTCs. The result indicated that 50 % of the captured cells can be detached from the substrate when the fluid shear stress was 180 dyn cm^{-2}. By integration of this CTCs capture nano-film with other single cell analysis device, we expected to further explore their applications in genome sequencing based on the captured CTCs.

Keywords Microfluidics · TiO_2 nanoparticles · Biocompatible · Circulating tumor cells

Electronic supplementary material The online version of this article (doi:10.1007/s10544-013-9781-9) contains supplementary material, which is available to authorized users.

R. He · Y. Liu · N. Zhang · Z. He · B. Cai · S. Li · W. Liu · S. Guo · X.-Z. Zhao (✉)
Key Laboratory of Artificial Micro- and Nano-structures of Ministry of Education, School of Physics and Technology, Wuhan University, Wuhan 430072, China
e-mail: xzzhao@whu.edu.cn

B. Cheng · B. Xiong (✉)
Zhongnan Hospital of Wuhan University, Hubei key laboratory of Tumor Biological behaviors, Hubei Cancer Clinical Study Center, Wuhan 430071, China
e-mail: binxiong88@yahoo.com

L. Zhao
Beijing National Laboratory for Molecular Sciences, Key Laboratory of Molecular Nanostructures and Nanotechnology, Institute of Chemistry, Chinese Academy of Sciences, Beijing 100190, China

L. Zhao
Department of Molecular and Medical Pharmacology, University of California Los Angeles (UCLA), 570 Westwood Plaza Building 114, Los Angeles 90095, CA, USA

Y. Chen
Department of Chemistry, Ecole Normale Superieure, 24 rue Lhomond, 75231 Paris, France

1 Introduction

Circulating tumor cells (CTCs) are the cells which detached from the primary tumors and enter into the blood circulation, emerging as novel tumor biomarkers and providing unique information for the cancer patients (Cristofanilli et al. 2004; Danila et al. 2011; Kling 2012; Lianidou and Markou 2011; Punnoose et al. 2010). The detection and monitoring of CTCs, is useful for the prognosis, prediction of response to therapy, or guiding clinical decision making for the patients with localized or metastatic disease, such as breast (Cristofanilli

et al. 2004; Lianidou and Markou 2011), prostate (Okegawa et al. 2008) and colorectal (Cohen et al. 2009; Lankiewicz et al. 2008) cancers. Researchers have reported that the number of CTCs in patients' peripheral blood can be used as an indicator of clinical outcomes (Cohen et al. 2009; Cristofanilli et al. 2004). In the case of breast cancer, patients with equal or more than 5 CTCs in 7.5 mL patient blood sample was indicative of clinical progression (Cristofanilli et al. 2004). Since the CTCs are related to the solid tumors, they can represent an enrichment of biomarker, which offer a distinct advantage over single biomarker detected by the conventional method, such as plasma DNA. Beyond counting the CTCs, new areas of research are directed toward developing novel sensitive assays for CTCs molecular characterization, which is very important for the future use of CTCs as targets of novel therapies and some mechanisms of cancer (Kling 2012). Recently, the captured CTCs had been subjected to the assays for subtype markers and mutations utilizing fluorescence *in situ* hybridization (FISH) (Lim et al. 2012) or polymerase chain reaction (Maheswaran et al. 2008; Powell et al. 2012).

However, the CTCs should be captured and isolated from the patient blood before any molecular characterization processed. It should be noted that the numbers of CTCs in the patient's blood with metastatic cancer are extremely low, from a few to hundreds CTCs in 1 mL blood (Cristofanilli et al. 2004; Nagrath et al. 2007). It is a technically tremendous challenge to capture, isolate and identify CTCs from the enormous quantity of other blood cells (10^9 mL^{-1}) in peripheral blood. Researchers have developed many technologies to capture and isolate CTCs, such as size-based microfiber devices (Hosokawa et al. 2010; Lim et al. 2012), magnetic beads-based immunomagnetic separation (Hoshino et al. 2011; Kang et al. 2012; Powell et al. 2012), electrical biosensor (Chung et al. 2011), different architecture microfluidic chip-based technologies (Adams et al. 2008; Bichsel et al. 2012; Hyun et al. 2013; Nagrath et al. 2007; Sheng et al. 2012; Stott et al. 2010; Wan et al. 2011; Wang et al. 2011), and nanomaterial based static capturing technologies (Wang et al. 2009; Zhang et al. 2012). Dimension advantage makes microfluidic devices a powerful tool in CTCs related studies, for providing not only larger surface area but also accurate flow control. Therefore, the CTCs recovery efficiency in microfluidic chips can be up to 95 %, which is superior to the FDA-approved CellSearch™ method (Wang et al. 2011). However, *in-situ* culture of captured CTCs in microfluidic device is still a great challenge since the limited channel volume usually obstructs the nutrient supply. Therefore an open-style CTCs capture and culture device is very attractive for routinely CTCs culture studies.

Nanomaterial based open-style static CTCs capturing technologies can be a promising method to solve the problem. Due to the nanoscale components on the cancer cell surface, such as microvilli and filopodia, nanostructure of the substrate can enhance the local topographic interaction between the cells and substrate, which improves the CTCs capture efficiency (Park et al. 2012; Wang et al. 2009; Zhang et al. 2012). For example, vertically oriented silicon nanopillars substrate coated with anti-epithelial-cell adhesion-molecule (EpCAM) antibody had been demonstrated to have outstanding cell capture efficiency in both static and dynamic systems (Wang et al. 2011, 2009). Gold clusters embedded on silicon nanowires for CTCs capturing was also reported (Park et al. 2012). On the other hand, horizontally packed ultra-long TiO_2 nanofibers were electrospun on the silicon substrate and successfully applied in the detection of CTCs in patient peripheral blood (Zhang et al. 2012). However, the silicon substrate was nontransparent, which is unfavorable for inverted microscope. Moreover, it was difficult to quantify the surface characteristics of the nanopillars or nanofibers based substrate, such as the surface roughness. Therefore, the capture-agent functionalized poly(3,4-ethylenedioxy)thiophenes (PEDOTs) nanodots were used to enhance the cancer cells capturing efficiency due to the synergistic effect between the nanostructures and ligand (Sekine et al. 2011). The size and density of PEDOT-COOH mandates can be easily controlled by the applied electropolymerized voltage, resulting in different surface roughness from 2 to 41 nm. It was shown that the cell capturing efficiency was highest with the surface roughness of 36 nm. The surface roughness has a positive effect on the CTCs capturing. However, the range of controllable surface roughness was small and the substrate was not suitable for high throughput fabrication. The size of the cancel cell surface components ranged from 80 to 300 nm. So, it is necessary to investigate the cell capturing on the larger surface roughness of substrate.

Herein, based on our previous work, a biocompatible and surface roughness controllable nano-film composed of TiO_2 nanoparticles was fabricated for highly efficient CTCs capture and *in-situ* identified by immunocytochemistry. The nano-film was coated with anti-EpCAM antibody for specific capturing EpCAM positive cancer cells. Compared to the substrate with TiO_2 nanofibers as we reported before (Zhang et al. 2012), the TiO_2 nanoparticles substrate can also significantly enhance the topographic interaction between the nanoparticles and cancer cell surface. Finally, by using the nano-film substrate, CTCs from gastric or colorectal cancer patient peripheral blood samples were captured and *in-situ* identified through three-color immunocytochemistry method. We also investigated the cancer cells capture strength at the nano-bio interface through exposing the cells to fluid shear stress in microfluidic device. The advantages of our platform is that i) the thickness and surface roughness of the nano-film can be easily controlled; ii) the substrate was biocompatible and transparent, which is subjected to *in situ* identify the CTCs; iii) By implementation of single cell

analysis device, we expected that this CTCs capture nanofilm can be explored their applications in genome sequencing based on the captured single CTCs.

2 Materials and methods

2.1 Materials

Anhydrous ethanol, acetonitrile, terpino, ethyl cellulose, lauric acid, dimethylsulfoxide (DMSO) were purchased from Sinopharm Chemical Reagent Co., Ltd, China. Titanium (IV) isopropoxide(TIP,97 %), methylamine (50 % w/w in water), 3-mercaptopropyl-trimethoxysilane (95 %, MPTMS), N-y-maleimidobutyryloxy succinimide ester (4-Maleimidobutyric acid N-hydrosuccinimide, GMBS), Paraformaldehyde (PFA, 36 % in water), Triton X-100, Bovine serum albumin (BSA), Fluorescein diacetate (FDA), Normal goat serum and 4, 6-Diamidino-2-phenylindole dihydrochloride (DAPI) were purchased from Sigma-Aldrich. Streptavidin (SA), Tween-20, Fetal bovine serum (FBS) and 0.25 % Trypsin-EDTA (Gibco, 1×) were obtained from Invitrogen. Biotinylated anti-human EpCAM/TROP1 antibody (goat IgG) was obtained from R&D systems. Phycoerythrin conjugated Anti-cytokeratin antibody and Fluorescein conjugated anti-human CD45 antibody was purchased from BD Biosciences. Deionized water generated from a MILLI-Q system (Millipore, MA, USA) was used for the synthesis. Glass slides were subsequently cleaned by acetone and ethanol, followed by dried using compressed nitrogen.

2.2 Preparation of mesoporous TiO_2 nanoparticle

According to the published method, hierarchical TiO_2 spheres (TiSP) were synthesized through a two-step process of controlled hydrolysis and hydrothermal reaction (Chen et al. 2010; Chen et al. 2009; Kim et al. 2009). In order to fabricate the transparent TiO_2 nanoparticle thin film on glass substrate, 1.0 g synthesized TiSP was dispersed into a mixture of 0.05 g lauric acid, 0.2 g ethyl cellulose and 10.0 mL terpinol and ethanol mixture solution (v/v 1:1) to form slurry. The TiSP slurry can be diluted with ethanol to a concentration of 5 mg mL^{-1}. Then the slurry was spincoated onto the glass surface, followed by annealing at 500 °C for 15 min.

2.3 Characterization

The infrared spectra of TiO_2 nanoparticles after anneal was measured using a FTIR spectrometer (Nicolet iS10, Thermo) in the range of 4,000–525 cm^{-1} to detect the surface functional groups. The Raman spectra of TiO_2 nanoparticles after anneal was carried out using a Raman spectroscopy (HORIBA Jobin Yvon LabRAM HR). The laser excitation was 488 nm and the power was 15 mW. The morphology of the synthesized TiO_2 nanoparticles and its film on glass substrate was observed by Field Emission Scanning Electron Microscopy (SEM, Sirion FEG). The surface roughness of the TiO_2 nanoparticles film on glass substrate was characterized using Atomic Force Microscopy (AFM, SPM-9500J3, SHIMADZU). The transmittance of the CTCs capturing devices was measured by UV–vis spectrophotometer (UV-2550, SHIMADZU).

2.4 Surface modification with antibody

The method for antibody conjugated on TiO_2 nanofilm was given in supporting information. After triple rinsed with anhydrous ethanol, the TiO_2 NPF substrate was modified with 4 % (v/v) 3-mercaptopropyl- trimethoxysilane (MPTMS) in anhydrous ethanol at room temperature for 1 h. After treated with silane, the substrate was rinsed 3 times with anhydrous ethanol to remove the unbounded MPTMS. Then we coated the TiO_2 nanoparticle with coupling agent GMBS. Next, the substrate was incubated with 10 μg mL^{-1} of streptavidin (SA) at 4 °C overnight. Before used, the substrate was washed 3 times with PBS to remove excess streptavidin, 10 μL biotinylated anti-epithelial cell adhesion molecule antibody (anti-EpCAM) (10 μg mL−1 in PBS) was added and incubated at room temperature for 2 h.

2.5 Cell capture and detection

The anti-EpCAM antibody coated substrate was placed into a chamber of 24-well plate, then the 1 mL cell suspension was added into this well, stood for 1 h in a cell incubator (37 °C, 5 % CO_2, Thermo Forma series II, Thermo Scientific). Afterwards, the substrate was rinsing with PBS at least 3 times. Imaging and counting of the captured cells were performed with a CCD camera (DP72, Olympus, Tokyo, Japan) mounted on an inverted microscope (IX71, Olympus, Tokyo, Japan). Pictures of the captured cells on substrate were analyzed using IPP software (Media Cybernetics Inc., Silver Spring, USA).

2.6 PDMS microchip fabrication to investigate the antibody and antigen interaction

The microchannel chip was fabricated in polydimethylsiloxane (PDMS) using a standard soft lithography and replica molding method. The width and height of microchannel were 65 μm and 1 mm, respectively. The PDMS with microchannel was reversible bonding with glass substrate. Then the capillary force can drive then TiO2 nanoparticles slurry filled the microchannel. After baking at 70 °C for half hour, the PDMS was carefully peeled off from the glass substrate. The substrate with TiO2 nanoparticles on the surface was annealed at 500 °C for 15 min. Then the substrate was bonded with PDMS by oxygen plasma.

To investigate the antibody and antigen interaction in the cancer cells capture, fluid shear stress (τ_0) was applied on the cells captured in microchannel. The velocity of the PBS solution was controlled by a langer injection pump. τ_0 has a relation to the velocity of the fluid:

$$\tau_0 = (6\mu Q)\Big/ WH^2,$$

Where Q is the fluid flow velocity, μ is the viscosity of the PBS solution (~10^{-3} Pa • s), W and H are the width and height of the microchannel, respectively (Chen et al. 2013).

3 Results and discussion

As shown in Fig. 1(a), we had presented a new platform for rare circulating cancer cell detection based on mesoporous TiO_2 nanopaticles, which was coated with anti-EpCAM antibody via multistep modification (see Fig. S1 in supporting information). In this way, the EpCAM positive cancer cells can be specifically captured through the antigen-antibody interaction. To study the contribution of nanoparticles in the CTCs assay, the glass substrate was patterned with and without TiO_2 nanoparticles as shown in Fig. 1(b). The distance between the patterned TiO_2 nanoparticles film was 1 mm. The captured HCT116 cells were stained by DAPI. The results indicated that the number of cells captured on TiO_2 nanoparticles film was about 15 times more than that without TiO_2 nanoparticles film. Figure 1(c) and (d) showed the SEM of the cells captured on the TiO_2 nanoparticles film. The diameter of the TiO_2 nanoparticles can be controlled by the temperature and reaction time. The thickness of the TiO_2 nanoparticles film on glass substrate can be controlled by the concentration of TiO_2 nanoparticles in the slurry, the viscosity of slurry and the revolving speed during the spincoating. As shown in the Fig. S2, the thickness of the film can be from 100 to 350 nm corresponding to the concentration 10 to 100 mg mL^{-1}. However the transmittance was decreased with increase the thickness. When the thickness was 260~350 nm, the transmittance was only about 30 %. In order to achieve higher transmittance, we used the slurry with concentration of 10 mg mL^{-1}. After annealing, the surface roughness of the TiO_2 nanoparticles on glass substrate was characterized using AFM. The result indicated that substrates with surface roughness from 36 to 94 nm were fabricated (see Fig. S3 in the supporting information). The AFM and SEM images of the TiO_2 nanoparitcles on a glass substrate with a surface roughness of 85 nm were shown in

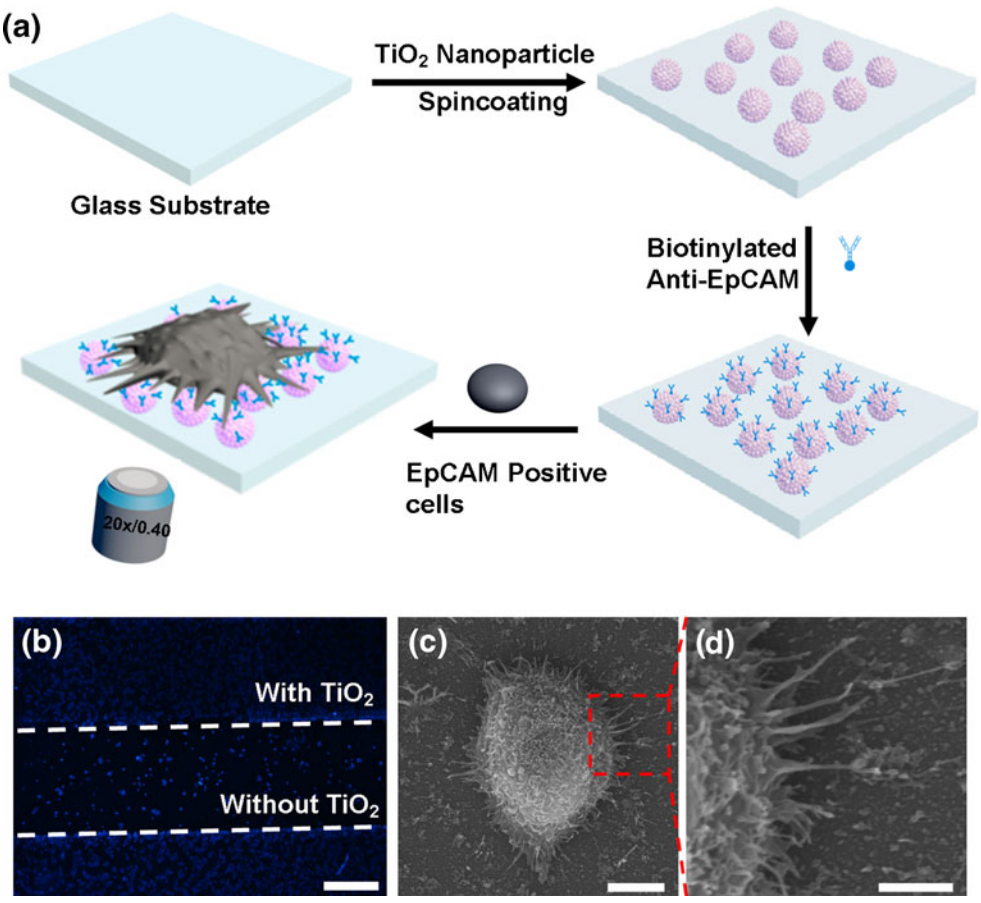

Fig. 1 **a** Schematic diagram of the biotinylated anti-EpCAM bioconjugated on TiO_2 nanoparticles for detecting EpCAM positive cancer cells. **b** The DAPI stain image micrograph of the HCT116 cells captured on the patterned with and without TiO_2 nanoparticles glass substrate. **c** The SEM image of the HCT116 cell captured on the TiO_2 nanoparticles glass substrate. **d** The SEM image of the microstructure topography of the cell in (**c**). The scale bar in b, c and d were 500, 5 and 2 μm, respectively

Fig. 2a, b. The insert in Fig. 2b was the SEM image of the as-synthesized TiO_2 nanoparticles with a diameter of ~ 400 nm. It was shown that the TiO_2 nanoparticles were almost single layer on the glass substrate, which exhibited two advantages: i) decrease the absorption of the fluorescence reagent; ii) increase the transmittance of the device compared to the thicker TiO_2 nanoparticles film. The transmittance of the TiO_2 nanoparticles on glass substrate with different surface roughness was shown in Fig. 2c. In the visible light band, the transmittance can achieve 80 %, which means that the device is transparent. The Fig. 2d gives a digital photograph of a transparent CTCs detection device with surface roughness of 85 nm.

In order to ensure successful antibody coating, FTIR and Raman spectroscopy were used to investigate the surface functional groups (see Fig. S4 in the supporting information). The FTIR spectra of TiO_2 nanoparticles after anneal shows the peaks corresponding to the stretching vibration of O-H and the deformation vibration of N-H around 3,500~3,200 cm^{-1} and 1,640~1,560 cm^{-1}, respectively. The result indicated that there exists hydroxide radical, which is also demonstrated through the Raman spectra. The biotinylated anti-EpCAM antibody can be successfully conjugated onto the TiO_2 nanoparticles via the chemical reaction illustrated in Fig. S1.

To understand the contribution of antibody coated on the TiO2 nanoparticles substrate, we design the following experiment. Cancer cells capture efficiencies of both anti-EpCAM coated substrate and bare TiO_2 substrate were conducted side by side using the same batch of HCT116 cell lines (See Fig. S4 in supporting information). The results indicated that antibody played a major role in the cancer cell immobilization, while the nanostructure alone could hardly lead to cell attachment.

In a proof experiment that the cancer cells were captured on the TiO_2 nanoparicles substrate through the antibody-antigen interaction, the EpCAM positive expression cancer cells (HCT116 cell line) was added onto the substrates with and without modified anti-EpCAM (see Fig. S4 in the supporting information). The results indicated that the density of captured cells on the anti-EPCAM modified substrate was about 9 times more than those of on the bare and only SA modified substrate, which means that the non-specific captured cells were almost negligible.

In order to investigate the effect of surface roughness of devices on the cell capture yields, CTCs capturing devices with surface roughness from 36 to 94 nm were used. To simulate the cells in cancer patient blood sample, different cancer lines were selected: EpCAM-positive cancer cell lines (such as colorectal cancer line HCT116, gastric carcinoma cell line MGC803) and EpCAM-negative cancer cell lines (such as cervical cancer line Hela and chronic myelogenous leukaemia cell line K562, corresponding to the adherent and suspension cell types, respectively). The cell concentration

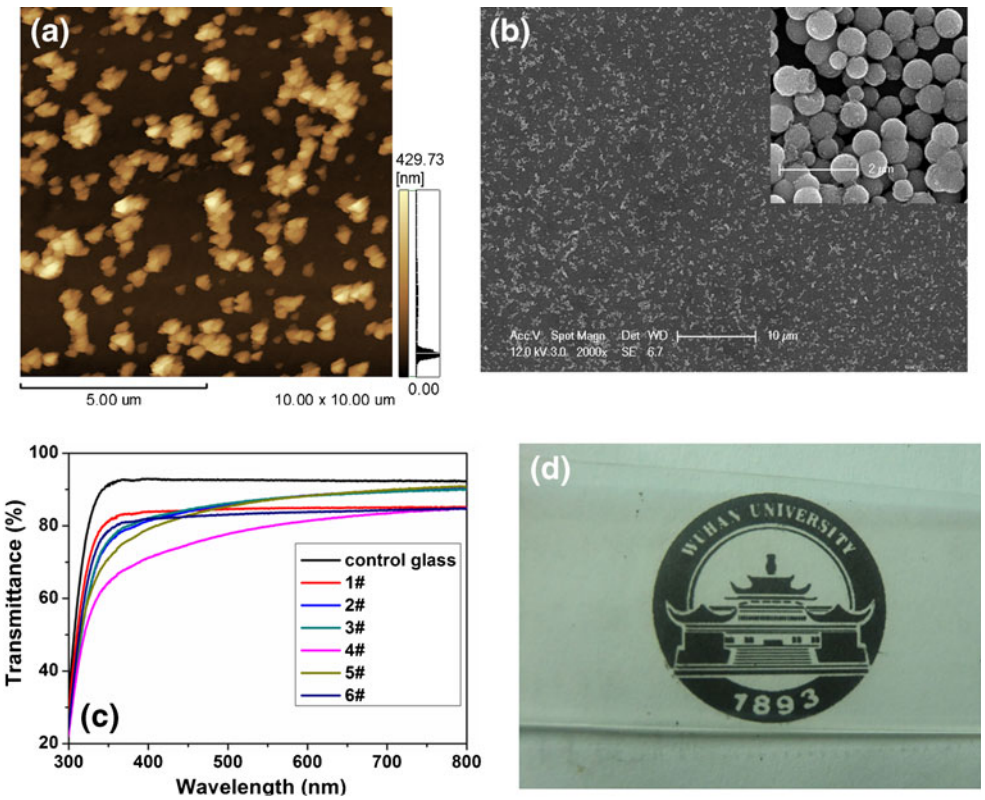

Fig. 2 The **a** AFM and **b** SEM images of the TiO_2 nanoparticles on glass substrate with the surface roughness of 85.4 nm. The insert in (**b**) is the SEM of TiO_2 nanoparticles after the hydrolysis and calcine of TiIP and methylamine. **c** is the transmittance of the TiO_2 nanoparticles substrate with different surface roughness. The 1# from 6# represent the devices with surface roughness around 36, 51, 60, 77, 85 and 94 nm, respectively. **d** is the digital photograph of the transparent TiO_2 nanoparticles on glass substrate. The diameter of the logo is about 2 cm. The scale bar in (**a**) and (**b**) are 2.5 and 2 μm, respectively

were the same for all the four cell lines, 1×10^5 ml^{-1}, and incubated 1 h in the incubator (37 °C, 5 % CO_2). As shown in Fig. 3a, the surface roughness really has an effect on the cells capture yields. For the EpCAM positive cancer cell lines, the device with surface roughness of 85 nm can reach the highest cells capture efficience. However, the EpCAM negative cancer cells capture yields were much lower, especially for the suspension cell line K562. When the surface roughness of the device was 85 nm, the capture yield of HCT116 cells can reach almost 13 times than that of K562. The effect of surface roughness on the cell capture yields can be attributed to the interaction between the mesoporous thin film and nanoscale components to the cell surface of the conical cells.

In order to investigate the effect of incubation time on the cell capture yield, the four cell lines mentioned above were incubated on the same device with surface roughness of 85 nm at different time, where the substrates were grafted with anti-EpCAM antibody. As shown in Fig. 3b, for the EpCAM positive cells, such as HCT116 and MGC803, the cell capture yields increased with the increasing incubation time and reached a maximal density at an incubation time of 1 h. On the contrary, relatively lower numbers of EpCAM-negative cells were captured, such as Hela and K562. The results indicated that it needed 1 h for the devices to capture all the cells in the sample. Therefore, the TiO_2 nanoparticles on glass substrate conjugated with anti-EpCAM was specific and sensitive for the EpCAM positive cell capturing.

Then we investigated the cancel cell capture efficiency using optimal capture condition. Different numbers of HCT 116 cells were spiked into PBS and healthy blood. The densities were approximately 20, 50, 100, 200, 250, 500 and 1,000 cells ml^{-1}, respectively. The captured cells were identified through the three-color immunocytochemisty method (details in the latter). As shown in Fig. 3c, more than 80 % of the cells spiked into PBS can be recovered and almost 50 % of the cells spiked into the artificial blood were recovered. The lower recovery efficience may be due to the interference of the higher density of blood cell. The cell recovery was comparable to the static cell capture based on silicon nanopillars (Wang et al. 2009) and TiO_2 nanofibers (Zhang et al. 2012) on silicon substrate.

Next, the TiO_2 nanoparticles based CTCs detection device was used to capture the rare CTCs in peripheral blood samples from colorectal or gastric cancer patients. The blood samples were obtained from the donator and preserved in blood collection tubes before use (containing EDTA). The substrate was about 1×1 cm and 1 mL blood sample was tested for each patient. The mononuclear cells in blood were separated from the whole blood using gradient centrifugation method. Then the sample was added onto an anti-EpCAM antibody conjugated TiO_2 nanoparticles substrate. After static capturing for 1 h and then rinsed by PBS, fixation, permeabilization and serum-free blocking solution agents were added onto the substrate for 10 min, respectively. Subsequently, the CTCs were identified and counted from non-specifically captured

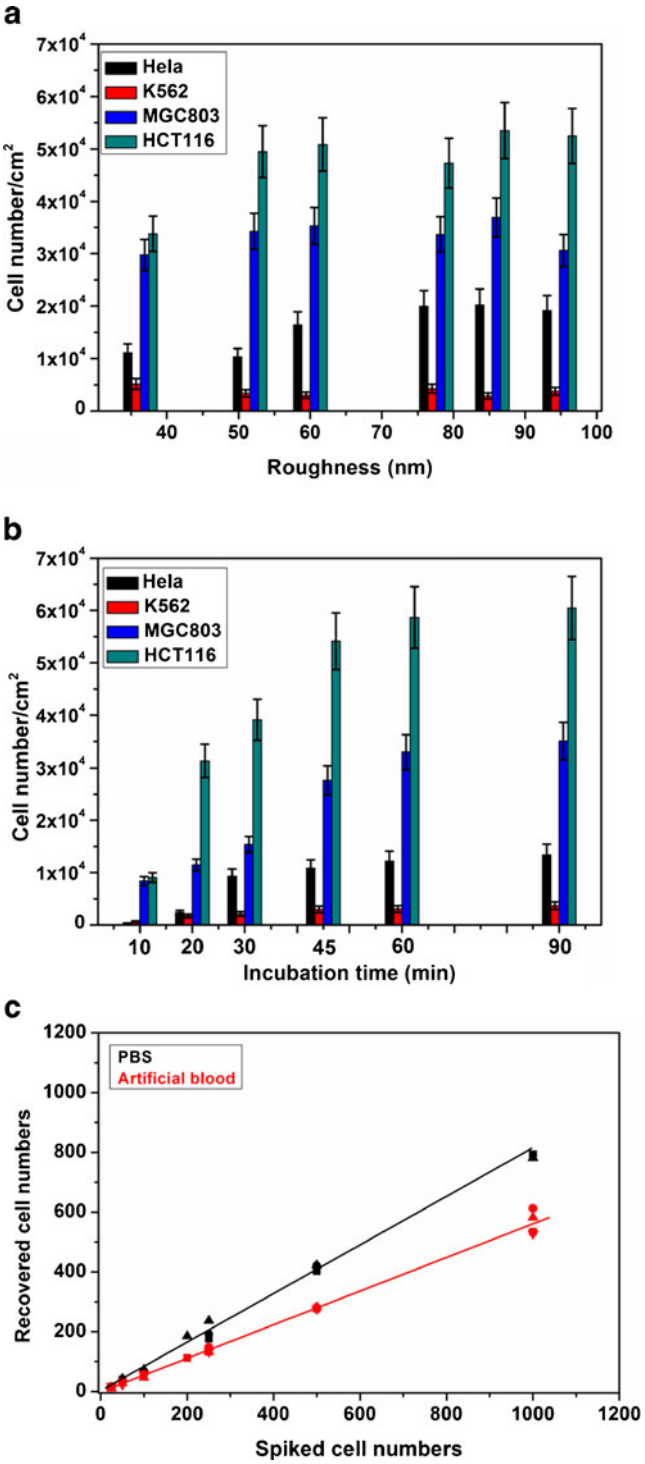

Fig. 3 Quantitative evaluations of the cancer cells capture yield (**a**) with different surface roughness TiO_2 nanoparticels on glass substrate ranging from 36 to 94 nm and (**b**) at different capture times. **c** is the recovery efficiencies of CTCs spiked different numbers ranging from 20 to 1,000 cells mL^{-1} in two types of samples: PBS and artificial human blood

white blood cells (WBCs) using commonly used three-color immunocytochemistry method, including PE-labeled anti-Cytokeratin (CK, a protein marker for epithelial cells), FITC-labeled anti-CD45 (a marker for WBCs) and DAPI for nuclear staining. As shown in Fig. 4, CTCs exhibit strong CK expression and WBCs present strong CD45 expression. After the combination of the images, the CTCs (CK+/CD45-/DAPI+) can be easily identified form WBCs (CK-/CD45+/DAPI+). In this way, CTCs ranging from 2 to 7 per milliliter are captured in the peripheral blood of the colorectal or gastric cancer patients. Therefore, the TiO_2 nanoparticles based CTCs detection device exhibited a considerable capture capacity.

There are some possible reasons attribute to superb cells capturing efficiency using nanomaterials. First of all, the local topographic interactions between nanomaterials and the nanoscale microvilli on cell surfaces can enhance the cell adhesive(Fischer et al. 2009). It is possible that the nanostructure can trigger the antigen clustering on the cell membrane to achieve a chelating effect, which can enhance the binding constant and efficiency(Sekine et al. 2011). Therefore, the cell capturing efficiency can reach a maximum when the surface roughness of the materials correlate with the average spacing of antigens. The nanoparticles on a substrate can alter the surface effects by change the surface roughness. Simulations of the nanoparticles interacting with synthetic membranes indicate that nanoscale surface roughness can greatly decrease repulsive interactions, such as electrostatic and hydrophilic. Therefore surface roughness can promote cell adhesion to substrate (Hoek and Agarwal 2006). On the other hand, the mechanical properties of materials may also be the crucial effect in cancer cells capturing (Sekine et al. 2011). The lower Young's modulus of the polymer nanodots, the higher cancer cells capturing. This may be attributed to the vacancy between the nanodots. The larger vacancy, the lower Young's modulus and the larger surface roughness. The Young's modulus of the polymer film may also have a relationship with the film thickness. The largest nanodots polymer film has a lowest Yong's modulus. At the nano-bio interface, there are some forces that can affect the cells adherent, such as long-range forces arising from van der Waals and repulsive electrostatic in electric double layer, or short-range forces arising from charge and steric and so on (Nel et al. 2009). However, it should be noted that the antibody and antigen interaction was also an important effect when we investigate the nanomaterials and cell interface interaction.

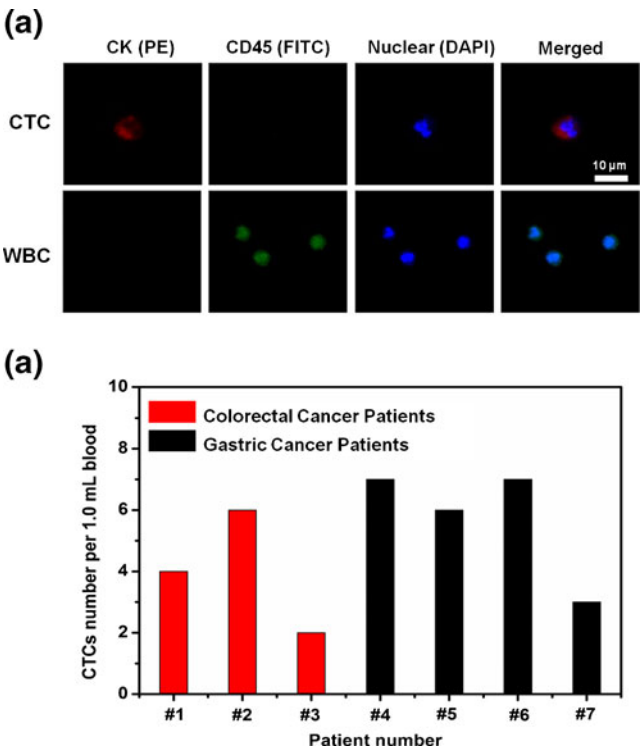

Fig. 4 Fluorescent micrographs of the CTCs captured from a gastric cancer patient peripheral blood sample. CTCs were identified from non-specifically trapped white blood cells on the TiO_2 nanoparticle substrate through three-color immuno-cytochemistry method based on PE-labeled anti-Cytokeratin antibody, FITC-labeled anti-CD45 antibody and DAPI nuclear staining. The scale bar is 10 μm. **b** The CTCs enumberation results obtained fromm 1.0 mL blood samples of colorectal (#1~#3) and gastric (#4~#7) cancer patients

In order to investigate the cancer cells capture strength at the nano-bio interface through exposing the cells to fluid shear stress in microfluidic device, we fabricated a microfluidic device where TiO_2 nanoparticles film was patterned in the micro-channel (See the Fig. 5(a) and S6 in supporting information). After the anti-EpCAm antibody was modified on TiO_2 nanoparticle film in the microchannel, the cancer cells (HCT116 cell line) was seeded inside the microchannel and incubated for 10 min. Then the cells were washed away by PBS at a controlled fluid velocity (Fig. 5(b)). If the device was not grafted with antibody, the cells can be easily washed away at a very low fluid shear stress (1.0 dyn cm^{-2}). However, the cells captured by antibody could withstand much larger fluid shear stress. As shown in Fig. 5(c), it was indicated that 50 % of the cancer cells can be detached from the microchannel when the fluid shear stress reached 180-dyne cm^{-2}, which indicated that the cancer cell capture strength by antibodies-cell interaction was larger than the nonspecific adhesion strength of cancer cells on the nano-rough surface (Chen et al. 2013). It also indicated that the antibody and antigen interaction was important when we investigate the effect of surface roughness on cancer capturing. Figure 5(d) ~ (f) shows the cell captured in the microchannel after washing with PBS at the fluid shear stress of 4, 180, 320 dyn cm^{-2} for 1 min, respectively. About 90 % of the captured HCT116 cells can be washed away when the fluid shear stress was 320 dyn cm^{-2}. Fortunately, The FDA stain result in Fig. 5(g) shows that the cells were still alive after washed with PBS. On the other hand, this is an alternate way

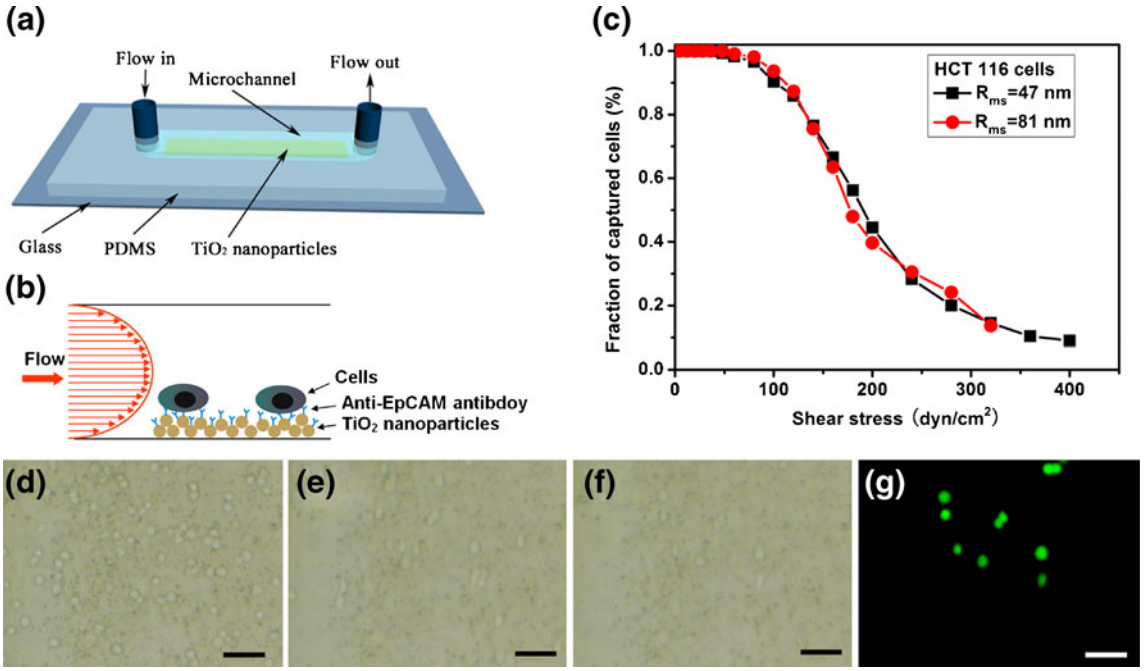

Fig. 5 Investigation of antibody and antigen interaction in microchannel. **a** Shows the microchip device, where the TiO_2 nanoparticles film was patterned in the microchannel. **b** The schematic of the cancer cells washed by fluid shear stress induced by fluid flow in microchannel. **c** Shows the fraction of captured cells in microchannel on two TiO_2 nanoparticles substrate (Rms=47 and 81 nm) after 1 min exposures to sustained directional fluid shear. **d** ~ **f** show the HCT116 cells captured in the microchannel (Rms=81 nm) after washed by PBS at the fluid shear stress of 4, 180, 320 dyn cm^{-2} for 1 min, respectively. **g** Shows the FDA stain result of cells after washed with PBS. The scale bar in **d** ~ **g** is 50 μm

to release captured cells, which is an interesting issue in CTCs research (Hou et al. 2013).

On the other hand, we also investigate the biocompatibility of the TiO_2 nanoparticles based CTCs detection device. The EpCAM positive HCT116 cells (1×10^5 ml^{-1}) were added on the device with surface roughness of 85.4 nm, which was conjugated with anti-EpCAM antibody. After incubated for 1 h in the cell incubator, the device was gently washed with PBS at least 5 times. Then the device with captured cells was incubated in the cell incubator. The Fig. 6(a) ~ (d) were the captured HCT116 cells incubated for 0, 1, 2 and 3 days, respectively. The results indicated that

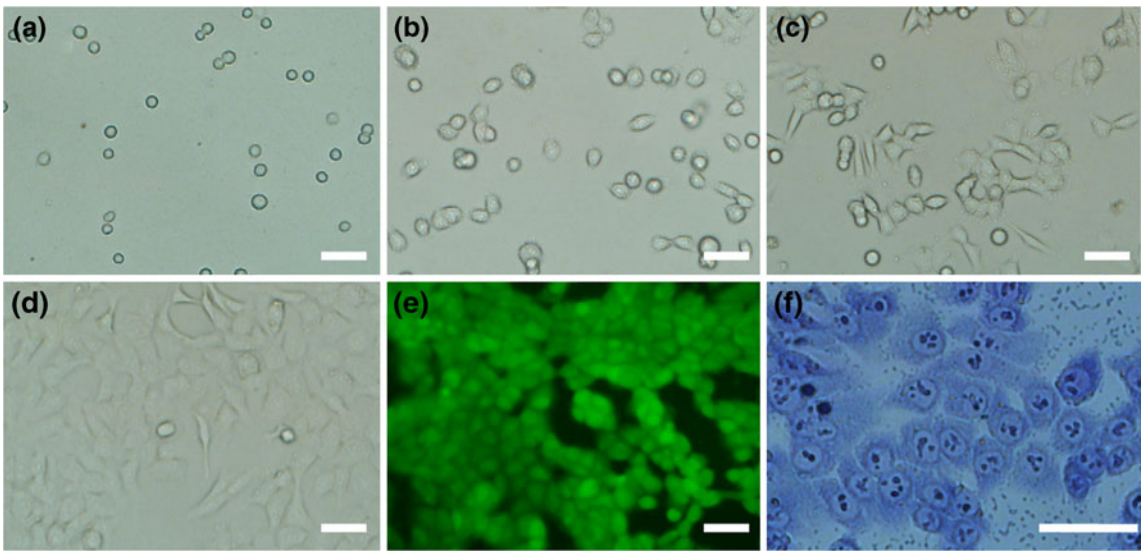

Fig. 6 The biocompatible of the TiO_2 Nanoparticle-Based Cell Capture device. **a** Shows the captured HCT116 cells; **b**, **c** and **d** were the cells incubated in a cell incubator (37 °C, 5 % CO_2) for 1, 2, 3 days, respectively; **e** was the cells stained by FDA after incubation; **f** was the cells stained by Wrights stain after incubation. The scale bar is 50 μm

the captured cells can be well cultured on the TiO_2 nanoparticles based substrate. The cell viability after cultured for 3 days was tested using FDA labelling (Fig. 6e). The green fluorescence represents the live cells. Moreover, the cytoplasm and nucleus of the captured cells after 3 days incubation can be distinguished through Wrights stain (Fig. 6f).

4 Conclusions

In conclusion, we demonstrated a new CTCs capture platform based on transparent and biocompatible TiO_2 nanoparticle spin coated on glass substrate conjugated with capture agent. The thickness and surface roughness of the TiO_2 nanoparticles film on glass substrate can be controlled by the concentration and viscosity of the TiO_2 nanoparitcles slurry, as well as the speed of the spin coating. The FTIR and Raman spectra demonstrated there exists hydroxide radical, which is utilized to conjugated antibody. The surface roughness of the devices have an effect on the cancer cells yields, which reached the maximum when the surface roughness is 85 nm among the devices. The enhanced local topographic interactions between the TiO_2 nanoparticles and extracellular matrix scaffolds, combined with the specific antigen-antibody interactions, we reliably recovered the spiked cancer cells in PBS and artificial blood samples. The devices were also utilized to capture and identify the rare CTCs from gastric cancer patient peripheral bloods using the three-color immunocytochemistry method. Compared to the nonspecific adhesion, the cancer cells captured through antibody-antigen interaction can withstand higher fluid shear stress in microfliudic device, which is very important for cancer cells rapidly capturing at the nano-bio interface. The cells can still be alive even washed at a very high fluid shear stress. Furthermore, the captured cells can be cultured on the devices, which demonstrating its good biocompatibility. Therefore, we expect that this CTCs capture device based on TiO_2 nanoparticles can be potentially applied in culturing the rare CTCs, molecular biological analysis of the CTCs, such as RT-PCR, FISH and gene sequence, and point-of care pharmacotherapy in the future.

Acknowledgement This research was partially supported by The National Basic Research Program (Grant No. 2011CB933300) and the National Natural Science Foundation of China (Grant Nos. 81272443, 51132001, J1210061 and 51272184). We thank Prof. Bin Xiong from the Oncology department of the Zhongnan Hospital of Wuhan University for providing the cancer patient blood samples and the normal blood samples

References

A.A. Adams, P.I. Okagbare, J. Feng, M.L. Hupert, D. Patterson, J. Gottert, R.L. McCarley, D. Nikitopoulos, M.C. Murphy, S.A. Soper, J. Am. Chem. Soc. **130**, 8633–8641 (2008)

C.A. Bichsel, S. Gobaa, S. Kobel, C. Secondini, G.N. Thalmann, M.G. Cecchini, M.P. Lutolf, Lab Chip **12**, 2313–2316 (2012)

D. Chen, L. Cao, F. Huang, P. Imperia, Y.-B. Cheng, R.A. Caruso, J. Am. Chem. Soc. **132**, 4438–4444 (2010)

D. Chen, F. Huang, Y.-B. Cheng, R.A. Caruso, Adv. Mater. **21**, 2206–2210 (2009)

W. Chen, S. Weng, F. Zhang, S. Allen, X. Li, L. Bao, R.H.W. Lam, J.A. Macoska, S.D. Merajver, J. Fu, ACS Nano **7**, 566–575 (2013)

Y.K. Chung, J. Reboud, K.C. Lee, H.M. Lim, P.Y. Lim, K.Y. Wang, K.C. Tang, H.M. Ji, Y. Chen, Biosens. Bioelectron. **26**, 2520–2526 (2011)

S.J. Cohen, C.J.A. Punt, N. Iannotti, B.H. Saidman, K.D. Sabbath, N.Y. Gabrail, J. Picus, M.A. Morse, E. Mitchell, M.C. Miller, G.V. Doyle, H. Tissing, L. Terstappen, N.J. Meropol, Ann. Oncol. **20**, 1223–1229 (2009)

M. Cristofanilli, G.T. Budd, M.J. Ellis, A. Stopeck, J. Matera, M.C. Miller, J.M. Reuben, G.V. Doyle, W.J. Allard, L.W.M.M. Terstappen, D.F. Hayes, N. Engl, J. Med. **351**, 781–791 (2004)

D.C. Danila, K. Pantel, M. Fleisher, H.I. Scher, Cancer J. **17**, 438–450 (2011)

K.E. Fischer, B.J. Alemán, S.L. Tao, R.H. Daniels, E.M. Li, M.D. Bunger, G. Nagaraj, P. Singh, A. Zettl, T.A. Desai, Nano Lett. **9**, 716–720 (2009)

E.M.V. Hoek, G.K. Agarwal, J. Colloid Interf Sci. **298**, 50–58 (2006)

K. Hoshino, Y.Y. Huang, N. Lane, M. Huebschman, J.W. Uhr, E.P. Frenkel, X.J. Zhang, Lab Chip **11**, 3449–3457 (2011)

M. Hosokawa, T. Hayata, Y. Fukuda, A. Arakaki, T. Yoshino, T. Tanaka, T. Matsunaga, Anal. Chem. **82**, 6629–6635 (2010)

S. Hou, H. Zhao, L. Zhao, Q. Shen, K.S. Wei, D.Y. Suh, A. Nakao, M.A. Garcia, M. Song, T. Lee, B. Xiong, S.-C. Luo, H.-R. Tseng, H.-h. Yu, Adv. Mater. **25**, 1547–1551 (2013)

K.-A. Hyun, K. Kwon, H. Han, S.-I. Kim, H.-I. Jung, Biosens. Bioelectron. **40**, 206–212 (2013)

J.H. Kang, S. Krause, H. Tobin, A. Mammoto, M. Kanapathipillai, D.E. Ingber, Lab Chip **12**, 2175–2181 (2012)

Y.J. Kim, M.H. Lee, H.J. Kim, G. Lim, Y.S. Choi, N.-G. Park, K. Kim, W.I. Lee, Adv. Mater. **21**, 3668–3673 (2009)

J. Kling, Nature Biotechnol. **30**, 578–580 (2012)

S. Lankiewicz, S. Zimmermann, C. Hollmann, T. Hillemann, T.F. Greten, Mol. Oncol. **2**, 349–355 (2008)

E.S. Lianidou, A. Markou, Clin. Chem. Lab. Med. **49**, 1579–1590 (2011)

L.S. Lim, M. Hu, M.C. Huang, W.C. Cheong, A.T.L. Gan, X.L. Looi, S.M. Leong, E.S.-C. Koay, M.-H. Li, Lab Chip **12**, 4388–4396 (2012)

S. Maheswaran, L.V. Sequist, S. Nagrath, L. Ulkus, B. Brannigan, C.V. Collura, E. Inserra, S. Diederichs, A.J. Iafrate, D.W. Bell, S. Digumarthy, A. Muzikansky, D. Irimia, J. Settleman, R.G. Tompkins, T.J. Lynch, M. Toner, D.A. Haber, N. Engl, J. Med. **359**, 366–377 (2008)

S. Nagrath, L.V. Sequist, S. Maheswaran, D.W. Bell, D. Irimia, L. Ulkus, M.R. Smith, E.L. Kwak, S. Digumarthy, A. Muzikansky, P. Ryan, U.J. Balis, R.G. Tompkins, D.A. Haber, M. Toner, Nature **450**, 1235–1239 (2007)

A.E. Nel, L. Madler, D. Velegol, T. Xia, E.M.V. Hoek, P. Somasundaran, F. Klaessig, V. Castranova, M. Thompson, Nature Mater. **8**, 543–557 (2009)

T. Okegawa, K. Nutahara, E. Higashihara, J. Urology **180**, 1342–1347 (2008)

G.-S. Park, H. Kwon, D.W. Kwak, S.Y. Park, M. Kim, J.-H. Lee, H. Han, S. Heo, X.S. Li, J.H. Lee, Y.H. Kim, J.-G. Lee, W. Yang, H.Y. Cho, S.K. Kim, K. Kim, Nano Letters **12**, 1638–1642 (2012)

A.A. Powell, A.H. Talasaz, H. Zhang, M.A. Coram, A. Reddy, G. Deng, M.L. Telli, R.H. Advani, R.W. Carlson, J.A. Mollick, S. Sheth,

A.W. Kurian, J.M. Ford, F.E. Stockdale, S.R. Quake, R.F. Pease, M.N. Mindrinos, G. Bhanot, S.H. Dairkee, R.W. Davis, S.S. Jeffrey, PLoS ONE **7**, e33788 (2012)

E.A. Punnoose, S.K. Atwal, J.M. Spoerke, H. Savage, A. Pandita, R.-F. Yeh, A. Pirzkall, B.M. Fine, L.C. Amler, D.S. Chen, M.R. Lackner, PLoS ONE **5**, e12517 (2010)

J. Sekine, S.-C. Luo, S. Wang, B. Zhu, H.-R. Tseng, H.-h. Yu, Adv. Mater. **23**, 4788–4792 (2011)

W. Sheng, T. Chen, R. Kamath, X. Xiong, W. Tan, Z.H. Fan, Anal. Chem. **84**, 4199–4206 (2012)

S.L. Stott, C.H. Hsu, D.I. Tsukrov, M. Yu, D.T. Miyamoto, B.A. Waltman, S.M. Rothenberg, A.M. Shah, M.E. Smas, G.K. Korir, F.P. Floyd, A.J. Gilman, J.B. Lord, D. Winokur, S. Springer, D. Irimia, S. Nagrath, L.V. Sequist, R.J. Lee, K.J. Isselbacher, S. Maheswaran, D.A. Haber, M. Toner, Proc. Natl. Acad. Sci. U.S. A. **107**, 18392–18397 (2010)

Y. Wan, J. Tan, W. Asghar, Y.-T. Kim, Y. Liu, S.M. Iqbal, J. Phys, Chem. B **115**, 13891–13896 (2011)

S.T. Wang, K. Liu, J.A. Liu, Z.T.F. Yu, X.W. Xu, L.B. Zhao, T. Lee, E.K. Lee, J. Reiss, Y.K. Lee, L.W.K. Chung, J.T. Huang, M. Rettig, D. Seligson, K.N. Duraiswamy, C.K.F. Shen, H.R. Tseng, Angew. Chem. Int. Ed. **50**, 3084–3088 (2011)

S.T. Wang, H. Wang, J. Jiao, K.J. Chen, G.E. Owens, K.I. Kamei, J. Sun, D.J. Sherman, C.P. Behrenbruch, H. Wu, H.R. Tseng, Angew. Chem. Int. Ed. **48**, 8970–8973 (2009)

N. Zhang, Y. Deng, Q. Tai, B. Cheng, L. Zhao, Q. Shen, R. He, L. Hong, W. Liu, S. Guo, K. Liu, H.-R. Tseng, B. Xiong, X.-Z. Zhao, Adv. Mater. **24**, 2756–2760 (2012)